

## Evidence of electronic confinement in pseudomorphic Si/GaAs superlattices

Vincenzo Spagnolo and Gaetano Scamarcio\*

*Dipartimento di Fisica and INFM, Università di Bari, I-70126 Bari, Italy*

Raffaele Colombelli,<sup>†</sup> Jean-Marc Jancu, and Fabio Beltram  
*Scuola Normale Superiore and INFM, I-56126 Pisa, Italy*

Lucia Sorba,<sup>‡</sup> Bernhard Meüller, and Alfonso Franciosi<sup>§</sup>  
*Laboratorio TASC-INFM, Padriciano 99, I-34012 Trieste, Italy*

(Received 8 April 1998)

We report the observation of coupling between intersubband plasmons and longitudinal-optical phonons in Si/GaAs superlattices pseudomorphically grown on GaAs-(001). Measurement of both phononlike ( $I_-$ ) and plasmonlike ( $I_+$ ) coupled modes by Raman scattering unambiguously demonstrated electronic confinement within pseudomorphic Si layers and allowed us to determine the  $0 \rightarrow 1$  intersubband transition energy. Comparison with the results of tight-binding calculations indicated a type-I band alignment across the Si/GaAs heterojunctions, with a conduction-band offset of 0.61 eV and a valence-band offset of 0.25 eV. [S0163-1829(98)52224-2]

The successful synthesis of Si/GaAs superlattices (SL's) has opened the way to the investigation of a prototype system with heterovalent lattice-mismatched interfaces.<sup>1-7</sup> Interest in this material configuration stems, in general, from the structural analogies and electronic differences relative to the Si-Ge system and, in particular, from the opportunity of studying interfaces between a covalent and a polar semiconductor.<sup>8-11</sup> For example, the band offset is expected to be strongly influenced by the interface termination in heterovalent heterojunctions with polar orientation,<sup>10,11</sup> and particularly in Si/GaAs SL's.<sup>8,9</sup>

Quantum confinement of optical phonons in Si/GaAs SL's has also been demonstrated,<sup>3,4</sup> but electronic confinement has not yet been reported. Observation of the latter hinges on the numerical values of the conduction- and valence-band discontinuities and would allow us to test theoretical predictions of the electronic structure of strained heterovalent heterojunctions.<sup>8-11</sup>

We report here the observation of coupled modes arising from two-dimensional (2D) plasmons associated with intersubband transitions in Si quantum wells (QW's) and GaAs longitudinal-optical (LO) phonons. Our results provide the first evidence that Si layers in Si/GaAs SL's can act as electronic potential wells. From the Raman shift of the coupled modes we obtained the  $0 \rightarrow 1$  intersubband-transition energy and the sheet-carrier densities with no additional parameters. Comparison with the results of tight-binding calculations allowed us to estimate the conduction- and valence-band discontinuities between Si and GaAs.

(Si)<sub>m</sub>/(GaAs)<sub>n</sub> SL's (Ref. 12) were grown by solid-source molecular-beam epitaxy on GaAs-(001) wafers under a constant As flux following the procedure described in Ref. 2. Structural investigation of Si/GaAs SL's by x-ray diffraction,<sup>1,2,5,6</sup> Raman scattering,<sup>3,4</sup> and transmission electron microscopy<sup>7</sup> have demonstrated that such a procedure achieved pseudomorphic growth of homogeneous Si and GaAs layers with relatively abrupt interfaces and long-range

periodicity. On the other hand, local-mode Raman spectroscopy<sup>3,4</sup> and Hall measurements have demonstrated the presence of Si out diffusion into the GaAs matrix where Si behaves as a donor impurity, and this may also affect electron confinement. Therefore we also grew, for comparison, multiple  $\delta$ -doped structures using Si coverage of 0.05 monolayer (ML) for each  $\delta$  layer, a Si growth temperature of 540 °C, a Si deposition rate of 22 ML/h, and an As equivalent pressure of  $3 \times 10^{-8}$  Torr. Structural and electrical data for the different samples are listed in Table I.

Raman experiments were performed at room temperature in backscattering configuration from the (001) surface, using several lines of an Ar<sup>+</sup> laser. We used an excitation power density of  $\sim 90$  kW/cm<sup>2</sup>, corresponding to an estimated photoexcited carrier density  $< 10^{17}$  cm<sup>-3</sup>. The latter is negligible with respect to the equilibrium electron density of our samples ( $n \geq 5 \times 10^{18}$  cm<sup>-3</sup>, see Table I). The scattered light was dispersed by a Jobin Yvon T64000 triple spectrometer, equipped with charge-coupled device (CCD) detection. The spectral resolution is 0.6 cm<sup>-1</sup>. Raman selection rules were checked by inserting a polarizer in front of the entrance slit of the monochromator.

Figures 1(a) and 1(b) show the Raman spectra of a (Si)<sub>0.05</sub>/(GaAs)<sub>35</sub> multiple  $\delta$ -doped sample<sup>13</sup> (sample 1). The peak at 291.2 cm<sup>-1</sup> in Fig. 1(a) is due to scattering by GaAs LO phonons. A structure in the range 500–580 cm<sup>-1</sup> in Fig. 1(b) is characteristic of second-order scattering processes by two GaAs optical phonons. The highest peak at 268.7 cm<sup>-1</sup> in Fig. 1(a) and the broadband centered at 837 cm<sup>-1</sup> in Fig. 1(b) are linked to the lower branch ( $\omega_-$ ) and the higher branch ( $\omega_+$ ) of coupled plasmon-LO phonon modes, respectively.

The V-shaped space-charge potential wells associated with *isolated*  $\delta$ -doped layers produce strong 2D electron confinement and create electronic subbands.<sup>14</sup> This substantially modifies the energy spectrum of coupled plasmon-phonon excitations.<sup>15,16</sup> However, when the spacing between  $\delta$ -

TABLE I. Details of the investigated samples. Layer thickness were checked by x-ray and Raman measurements and are given in monolayer units (ML) (Ref. 12).  $I_-$  and  $I_+$  are the energies of intersubband plasmon–LO-phonon modes measured by Raman scattering.  $\omega_{01}$  and  $n_s$  (Raman) are the 0→1 intersubband transition energy and the sheet-carrier density inferred from  $I_-$  and  $I_+$  without external parameters as described in the text.  $n_s$  (Hall) is the sheet-carrier density as determined by Hall experiments. For sample 1 in which a 3D charge distribution is present, the plasmon-phonon mode energies ( $\omega_{\pm}$ ) and the bulk electronic density ( $n$ ) are listed.

Sample	Si/GaAs (ML)	Number of periods	$I_-$ ( $\text{cm}^{-1}$ )	$I_+$ ( $\text{cm}^{-1}$ )	$\omega_{01}$ (MeV)	$n_s$ ( $\text{cm}^{-2}$ ) (Raman)	$n_s$ ( $\text{cm}^{-2}$ ) (Hall)
2	3/50	15	282.8	1095	109.6	$1.2 \times 10^{13}$	$1.4 \times 10^{13}$
3	2/35	10	287	816	89.9	$5.6 \times 10^{12}$	$4 \times 10^{12}$
4	2/35	10	287.8	810	91	$4.9 \times 10^{12}$	$4 \times 10^{12}$
5	2/28	15	287.5	823	91.7	$5.3 \times 10^{12}$	
1	0.05/35	10	$\omega_- = 268.7$	$\omega_+ = 837$		$n = 8.5 \times 10^{18} \text{ cm}^{-3}$	$n = 8 \times 10^{18} \text{ cm}^{-3}$

doped layers is reduced below  $\sim 200$  Å and the sheet-carrier density is larger than  $\sim 10^{12} \text{ cm}^{-2}$ , the strong coupling between subbands originally localized in separate potential wells leads to wave-function delocalization, miniband formation, and spreading of the electronic density.<sup>17</sup> Therefore, plasmons in short period *multiple*  $\delta$ -doped samples are quasi-three dimensional in nature<sup>18</sup> and consequently the associated Raman spectra are very similar to those of homogeneously  $n$ -doped GaAs at high doping level.<sup>19</sup> These considerations apply well to sample 1, in which the spacing between the  $\delta$ -doped layers is 100 Å. From the measured  $\omega_-$  and  $\omega_+$  energies we estimated a 3D carrier density  $n = 8.5 \times 10^{18} \text{ cm}^{-3}$ . This value compares well with that of  $8 \times 10^{18} \text{ cm}^{-3}$  derived from Hall measurements (see Table I).

Figures 1(c) and 1(d) show the Raman spectra of the  $(\text{Si})_3/(\text{GaAs})_{50}$  SL (sample 2). Besides one-phonon and two-phonon GaAs bands analogous to those observable in Figs. 1(a) and 1(b), additional structures ascribed to Si-related phonons are present. The band centered at  $386 \text{ cm}^{-1}$  is due to a superposition of Si-derived local vibrational modes (LVM).<sup>20,21</sup> This observation and Hall measurements (see Table I) demonstrate the occurrence of relevant diffusion of Si ions into the GaAs matrix. On the other hand, observation of the characteristic band due to Si-like LO confined

phonons at  $477 \text{ cm}^{-1}$ , labeled Si on Fig. 1(d), demonstrates that the vast majority of the Si atoms remain localized in the pseudomorphic layers, yielding an overall composition profile close to the nominal one.<sup>3</sup>

The peak at  $282.8 \text{ cm}^{-1}$  in Fig. 1(c) and the broadband at  $1095 \text{ cm}^{-1}$  in Fig. 1(d) are related to the lower ( $I_-$ ) and the higher ( $I_+$ ) branches of the intersubband plasmon–LO-phonon coupled excitations. The 2D nature of these coupled modes is unambiguously demonstrated by the energy position of the  $I_-$  and  $I_+$  bands. The  $I_-$  band position falls in the wave-number range between the transverse-optical (TO) and the LO phonons. This would be consistent with a three-dimensional plasmon-phonon mode only in the presence of Landau damping, i.e., for a  $n < 2 \times 10^{18} \text{ cm}^{-3}$  carrier density.<sup>19</sup> However, the experimental position of the higher plasmon-phonon branch would then require  $n > 10^{19} \text{ cm}^{-3}$ , so that there is no way to explain at the same time the position of the two bands with 3D plasmon-phonon modes. The 2D nature of the  $I_-$  and  $I_+$  modes remains the only viable explanation. Similar features associated with Si-related phonons and 2D intersubband plasmon-phonon excitations were observed in all investigated SL samples. The results are summarized in Table I.

The energies  $I_{\pm}$  of the intersubband plasmon–LO-phonon coupled modes are determined by the zeros of the real part of

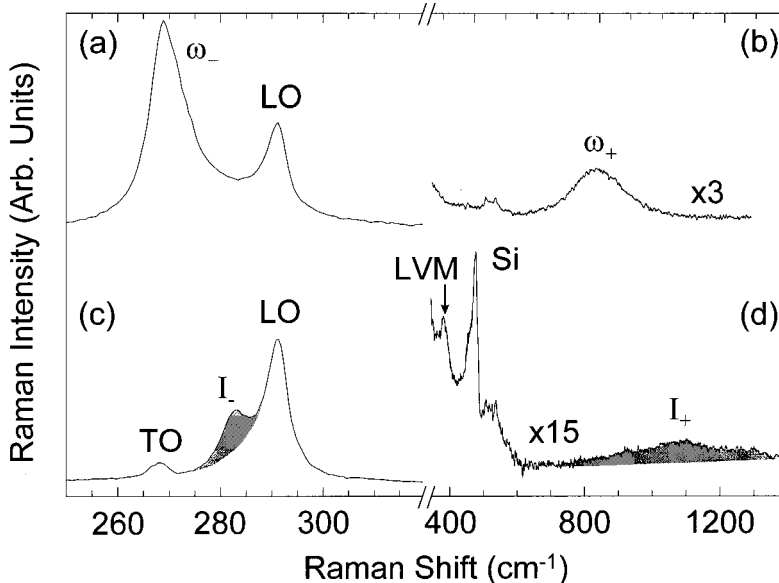


FIG. 1. Raman spectra of samples 1 (a,b) and 2 (c,d). Bands marked  $\omega_{\pm}$  on traces a,b are linked to 3D plasmon–LO-phonon coupled modes. Shaded bands labeled  $I_{\pm}$  on traces c,d correspond to intersubband plasmon–LO-phonon coupled modes. TO (LO) on traces a,c label the transverse (longitudinal) optical GaAs phonons. LVM and Si on trace d mark Si-related local vibrational modes in GaAs and confined phonons in Si quantum wells, respectively.

the dielectric function. Considering only transitions between the first and second subbands (0→1) and neglecting the population of the excited subbands, the dielectric function can be written as

$$\begin{aligned} \varepsilon(\omega) = & \varepsilon_\infty + \varepsilon_\infty \left( \frac{\omega_{\text{LO}}^2 - \omega_{\text{TO}}^2}{\omega_{\text{TO}}^2 - \omega^2 - i\gamma\omega} \right) \\ & + \varepsilon_\infty \left( \frac{\Omega_{01}^2}{\omega_{01}^2 - \omega^2 - i\Gamma_{01}\omega} \right), \end{aligned} \quad (1)$$

where  $\varepsilon_\infty$  is the high-frequency dielectric constant,  $\omega_{\text{LO(TO)}}$  is the LO (TO)-phonon frequency,  $\gamma$  and  $\Gamma_{01}$  account for phonon damping and subband broadening;  $\Omega_{01}$  is the so-called depolarization shift and takes into account collective effects due to electron-electron scattering. For small in-plane components of the wave vector the following relation holds:  $\Omega_{01}^2 = 4\pi e^2 n_s L_{01} \omega_{01} / (\varepsilon_0 \varepsilon_\infty \hbar c)$ . A well-tested approximation of the Coulomb matrix element is  $L_{01} \sim 0.055 L_z (\text{\AA})$ , where  $L_z$  is the well width.<sup>22</sup> From the condition  $\varepsilon(\omega) = 0$  and neglecting damping effects ( $\gamma, \Gamma_{01} \rightarrow 0$ ) one obtains the energies of the coupled modes:

$$\begin{aligned} I_\pm^2 = & \frac{\omega_{\text{LO}}^2 + \omega_{01}^2 + \Omega_{01}^2}{2} \\ & \pm \frac{1}{2} [(\omega_{\text{LO}}^2 - \omega_{01}^2 - \Omega_{01}^2)^2 + 4\Omega_{01}^2(\omega_{\text{LO}}^2 - \omega_{\text{TO}}^2)]^{1/2}. \end{aligned} \quad (2)$$

Note that  $I_\pm$  depend on two parameters only:  $\omega_{01}$  and the sheet-carrier density  $n_s$ . Using the experimental  $I_\pm$  energies we estimated the  $\omega_{01}$  and  $n_s$  values reported in Table I. The good agreement between the  $n_s$  values obtained by the Raman spectra and those measured by Hall experiments confirm the validity of our analysis.

We address now the physical origin of the confining potential yielding 2D electron confinement in Si quantum wells. Owing to Si out diffusion in real Si/GaAs SL's the electronic potential profile will result from a combination of two contributions, namely, the crystal potential due to the pseudomorphic localized Si layers and the additional space-charge effect due to the Si donors. A full-blown calculation requires knowledge not only of the actual Si layers' thickness but also of Si donor distribution in the GaAs matrix. The latter cannot be easily obtained from structural probes such as x-ray diffraction (XRD) or TEM. However, calculations carried out modeling our samples as multiple  $\delta$ -doped structures, i.e., neglecting the crystal potential associated to pseudomorphic Si layers, show that the donor-related space-charge effects give only a relatively weak modulation of the electronic potential and no 2D confinement.

Accordingly, we calculated the band structure of our samples including only the periodic Si potential expected from the XRD- and TEM-determined composition profile. The band structure was obtained within an empirical tight-binding  $sp^3s^*d^5$  nearest-neighbor model including spin-orbit coupling.<sup>23</sup> Strain effects were taken into account assuming pseudomorphic growth and scaling the Si matrix elements of the QW Hamiltonian with respect to bond-angle distortions and bond-length changes. We obtained a Si band-gap reduction of 50% and a band-gap difference of 0.86 eV

TABLE II. Calculated 0→1 intersubband transition energies corresponding to a given conduction-band offset  $\Delta E_c$  value.

Si/GaAs (ML)	$\Delta E_c$ (eV)	$\omega_{01}$ (meV) (theory)
2/28	-0.66	108
	-0.61	92
	-0.56	77
2/35	-0.66	105
	-0.61	88
	-0.56	72
3/50	-0.71	122
	-0.68	110
	-0.66	98
	-0.61	75

between GaAs and Si at room temperature, consistent with the value of 081 eV proposed in Ref. 24 based on pseudopotential calculations by People<sup>25</sup> for pseudomorphic Si layers on Ge.

Table II shows the calculated  $\omega_{01}$  corresponding to different postulated values of the Si/GaAs conduction-band offset ( $\Delta E_c$ ). Good agreement with the experimental  $\omega_{01}$  values of Table I was found for  $\Delta E_c = -0.61$  eV in all samples but sample 2. The negative sign denotes that the conduction-band minimum of Si is lower than that of GaAs in the SL. For sample 2 better agreement was obtained with  $\Delta E_c = -0.68$  eV. This  $\sim 10\%$  difference is probably related to non-negligible space-charge effects in this sample, leading to increased electronic confinement and an apparent increase in  $|\Delta E_c|$  within our tight-binding model. In fact, sample 2 has a much larger spacing between Si layers and a  $n_s$  value a factor of 2 larger than that observed in the other SL's.

Using  $\Delta E_c = -0.61$  eV and the calculated value of the band-gap difference between the pseudomorphic Si layers on GaAs, we obtained a valence-band offset  $\Delta E_v = 0.25 \pm 0.05$  eV and a type-I band alignment, i.e., both the conduction-band minimum and the valence-band maximum occur within the Si layers in the SL. The above valence-band offset value is in agreement with the results of prior photoemission studies of Si/GaAs(001) heterojunctions, which yielded  $\Delta E_v = 0.39 \pm 0.10$  and  $\Delta E_v = 0.23 \pm 0.01$  eV.<sup>24-26</sup>

*Ab initio* calculations have shown that the valence-band maximum may fall either in Si or in GaAs layers in the SL, depending on the atomic configuration of the interface and the corresponding local interface dipole.<sup>8,9</sup> For example, for Si layers pseudomorphically strained on GaAs(001),  $\Delta E_v = 0.55$  eV is expected for a 50-50 Si-As termination within a single intermixed atomic plane at the interface (type A configuration in Refs. 9–11), while  $\Delta E_v = -0.10$  eV is expected for 50-50 Si-Ga termination within a single intermixed atomic plane at the interface (type B configurations in Refs. 9–11). More complex configurations leading to two Si-As and Si-Ga intermixed planes at the interface and no ionic dipole (configurations C-D in Refs. 9–11) would give  $\Delta E_v = 0.22-0.23$  eV, close to the average of the two previous values, and similar to the value of 0.21 eV expected for the nonpolar interface configuration.<sup>27</sup> Our experimental value for  $\Delta E_v$  clearly suggests that local atomic configura-

tions yielding no ionic dipole have been achieved at the Si/GaAs interface, although we caution the reader that only a few of the simplest possible interface configurations have been examined by theory in Refs. 8 and 9.

In conclusion, we reported the observation of  $I_-$  and  $I_+$

intersubband plasmon–LO-phonon modes in Si/GaAs superlattices. This allowed us to directly estimate the intersubband transition energy and the sheet-carrier density and obtain experimental evidence of electron confinement within Si quantum wells in Si/GaAs superlattices.

\*Electronic address: scamarcio@ba.infn.it

†Also at Istituto ICMAT del CNR, Montelibretti, Italy.

‡Electronic address: colombel@aix6sns.sns.it

§Also at Dipartimento di Fisica, Università di Trieste, I-34127 Trieste, Italy.

<sup>1</sup>H. J. Gillespie, G. E. Crook, and R. J. Matyi, *Appl. Phys. Lett.* **60**, 721 (1992).

<sup>2</sup>L. Sorba, G. Bratina, A. Franciosi, L. Tapfer, G. Scamarcio, V. Spagnolo, and E. Molinari, *Appl. Phys. Lett.* **61**, 1570 (1992).

<sup>3</sup>G. Scamarcio, V. Spagnolo, E. Molinari, L. Tapfer, L. Sorba, G. Bratina, and A. Franciosi, *Phys. Rev. B* **46**, 7296 (1992).

<sup>4</sup>G. Scamarcio, V. Spagnolo, E. Molinari, L. Tapfer, L. Sorba, G. Bratina, and A. Franciosi, *Superlattices Microstruct.* **12**, 429 (1992).

<sup>5</sup>L. Sorba, G. Bratina, A. Franciosi, L. Tapfer, G. Scamarcio, V. Spagnolo, A. Migliori, P. Merli, and E. Molinari, *J. Cryst. Growth* **127**, 121 (1993).

<sup>6</sup>H. J. Gillespie, J. K. Wade, G. E. Crook, and R. J. Matyi, *J. Appl. Phys.* **73**, 95 (1993).

<sup>7</sup>A. Franciosi, L. Sorba, G. Bratina, and G. Biasiol, *J. Vac. Sci. Technol. B* **11**, 1628 (1993).

<sup>8</sup>R. G. Dandrea, S. Froyen, and A. Zunger, *Phys. Rev. B* **42**, 3213 (1990).

<sup>9</sup>M. Peressi, L. Colombo, R. Resta, S. Baroni, and A. Baldereschi, *Phys. Rev. B* **48**, 12 047 (1993).

<sup>10</sup>G. Biasiol, L. Sorba, G. Bratina, R. Nicolini, A. Franciosi, M. Peressi, S. Baroni, R. Resta, and A. Baldereschi, *Phys. Rev. Lett.* **69**, 1283 (1992).

<sup>11</sup>For a recent review see, e.g., A. Franciosi and C. G. Van de Walle, *Surf. Sci. Rep.* **25**, 1 (1996).

<sup>12</sup>Subscripts  $m, n$  denote the layer thickness expressed in monolayers, defined as the distance between two adjacent Si atomic

planes (1.35 Å) or the distance between two subsequent Ga or As atomic planes (2.83 Å), in the case of Si and GaAs layers, respectively.

<sup>13</sup>The  $(\text{Si})_{0.05}/(\text{GaAs})_{35}$  notation indicates the fractional coverage (5% of a Si plane) employed for each  $\delta$  layer, i.e.,  $3 \times 10^{13} \text{ cm}^{-2}$  Si atoms. A review of  $\delta$  doping in semiconductors can be found in E. F. Schubert, *Doping in III-V Semiconductors* (Cambridge University Press, Cambridge, 1993).

<sup>14</sup>M. H. Degani, *Phys. Rev. B* **44**, 5580 (1991).

<sup>15</sup>A. Mlayah, R. Carles, E. Bedel, and A. Munoz-Yague, *Appl. Phys. Lett.* **62**, 2848 (1993).

<sup>16</sup>A. Mlayah, R. Carles, E. Bedel, and A. Munoz-Yague, *J. Appl. Phys.* **74**, 1072 (1993).

<sup>17</sup>M. H. Degani, *J. Appl. Phys.* **70**, 4362 (1991).

<sup>18</sup>R. C. Newman, M. J. Ashwin, M. R. Fahy, S. N. Holmes, C. Roberts, X. Zhang, and J. Wagner, *Phys. Rev. B* **54**, 8769 (1996).

<sup>19</sup>G. Abstreiter, M. Cardona, and A. Pinczuk, in *Light Scattering in Solids IV*, edited by M. Cardona and G. Guntherodt (Springer, Heidelberg, 1984), p. 5.

<sup>20</sup>M. Ramsteiner, J. Wagner, H. Ennen, and M. Maier, *Phys. Rev. B* **38**, 10 669 (1988).

<sup>21</sup>D. N. Talwar and M. Vandervyver, *Phys. Rev. B* **40**, 3799 (1989).

<sup>22</sup>G. Fishman, *Phys. Rev. B* **27**, 7611 (1983).

<sup>23</sup>J. M. Jancu, R. Scholtz, F. Beltram, and F. Bassani, *Phys. Rev. B* **57**, 6493 (1998).

<sup>24</sup>G. Bratina, L. Sorba, A. Antonini, L. Vanzetti, and A. Franciosi, *J. Vac. Sci. Technol. B* **9**, 2225 (1991).

<sup>25</sup>R. People, *Phys. Rev. B* **34**, 2508 (1986).

<sup>26</sup>R. S. List, J. C. Woicik, I. Lindau, and W. E. Spicer, *J. Vac. Sci. Technol. B* **5**, 1279 (1987).

<sup>27</sup>C. G. Van de Walle and R. M. Martin, *Phys. Rev. Lett.* **62**, 2028 (1989).